Contents   Author Index   Keyword Index

DATA-DRIVEN ALIGNMENT OF
3D BUILDING MODELS AND DIGITAL AERIAL IMAGES

J. Jung, C. Armenakis*, G.Sohn

Department of Earth and Space Science and Engineering
Geomatics Engineering, GeoICT Lab
York University, Toronto, Canada
{jwjung} {armenc} {gsohn}@yorku.ca

Commission VII, WG VII/6

KEY WORDS: Data fusion, registration, building models, digital image, similarity assessment, updating

ABSTRACT:

Various types of data taken from different sensors or from different viewpoints at different times are used to cover the same area. This abundance of heterogeneous data requires the integration and therefore the co-registration of these data in many applications, such as data fusion and change detection for monitoring of urban infrastructure and land resources. While many data registration methods have been introduced, new automatic methods are still needed due to increasing volumes of data and the introduction of new types of data. In addition, large-scale 3D building models have already been constructed for mapping or for generating 3D city models. These valuable 3D data can also be used as a geometric reference in sensor registration process. This paper addresses data fusion and conflation issues by proposing a data-driven method for the automatic alignment of newly acquired image data with existing large scale 3D building models. The proposed approach is organised in several steps: extraction of primitives in the 3D building model and image domains, correspondence of primitives, matching of primitives, similarity assessment, and adjustment of the exterior orientation parameters of the images. Optimal building primitives are first extracted in the existing 3D building model using a priority function defined by the orientation of building, complexity of building, inner angles of building, and building geometric type. Then the optimally extracted building primitives are projected into image space to be matched with extracted image straight lines data sets followed by a similarity assessment. For the initial localization, the straight lines extracted in the digital image are assessed in the search area based on their location with respect to the corresponding optimal building primitives. The location of the straight line having the highest score is determined. In that designated area location, new straight lines are extracted by weighting straight lines representing each vector of optimal building primitives. The corresponding vertices of the optimal building model are determined in the image by the intersection of straight lines. Finally, the EO parameters of the images are efficiently adjusted based on the existing 3D building model and any new image features can then be integrated in the 3D building model. An evaluation of the proposed method over various data sets is also presented.

1. INTRODUCTION

With the recent advancements in remote sensing technology, various types of data taken from different sensors or from different viewpoints at different times are used to cover the same area. This abundance of heterogeneous data requires the integration and therefore the co-registration of these different data sets in many applications such as detection of changes in the urban infrastructure and mapping of land resources. While many data registration methods have been introduced, new automatic methods are still needed due to the increasing volume of data and the introduction of new types of data. Zitova and Flusser, 2003 presented a comprehensive survey of image registration methods, while Fonseca and Manjunath, 1996 compared registration techniques for multisensory remotely sensed imagery and presented a brief discussion of each of the techniques. Habib et al., 2005 introduced alternative approaches for the registration of data captured by photogrammetric and lidar systems to a common reference frame. However, most studies aim to register images with other sensors data such as lidar and SAR data sets. Although large-scale 3D building

models have been already generated in Google Earth, of Google and Virtual Earth of Microsoft, the application of the building information is limited to a secondary role for text-based data search. However, these valuable 3D data can be also used as a geometric reference in sensor registration process. Therefore, this paper addresses data fusion and conflation issues by proposing a data-driven method for the automatic alignment of newly acquired image data with existing large scale 3D building models. Also, while existing 3D building models have inherent errors, in this study we assume that the existing 3D building models are free of any geometric errors and that the exterior orientation parameters of image are to be adjusted using the 3D building model as reference control data. This paper is organized into four parts. In section 2, we address the proposed new registration method, section 3 deals with the evaluation of the approach, and conclusions are given in section 4.

---

* Corresponding author.

In: Wagner W., Székely, B. (eds.): ISPRS TC VII Symposium – 100 Years ISPRS, Vienna, Austria, July 5–7, 2010, IAPRS, Vol. XXXVIII, Part 7B

Contents   Author Index   Keyword Index

2. REGISTRATION METHOD

To register the input digital image with existing 3D building models, geometric primitives in both data sets are extracted and their corresponding image coordinates are computed by a similarity assessment. The EO parameters of the images can be efficiently adjusted based on the corresponding image coordinates of primitives. Figure 1 illustrates the outline of our approach.
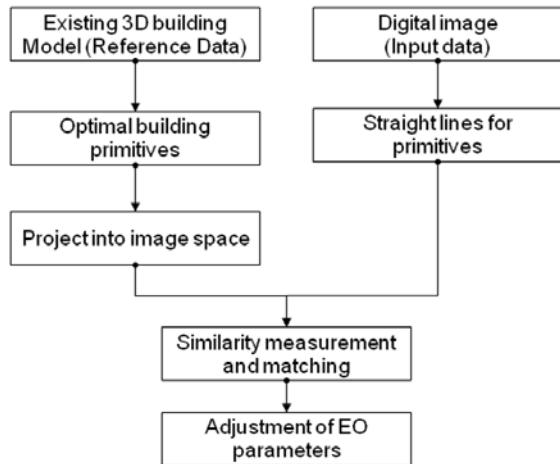

Figure 1. Flowchart of the alignment method

2.1 Feature extraction

2.1.1   Extraction of optimal building primitives

The 3D existing building models derived from various sensors have different accuracy according to generation method. Also, though the 3D building models may have been constructed by same method, all the 3D building models could not be used in the registration process. This is because their accuracy could be different depending on the skill of the operator and because use of the entire 3D building model for registration may be inefficient and time-consuming. We assume that simple buildings which satisfy a defined geometric condition of building are more useful for the registration process. For example, a building polygon which consists of 4 lines with 90 degree inner angles is likely to be a more general and efficient primitive because it is more difficult to describe complex buildings, since there is greater chance that the operator will misrepresent a complex. Therefore, it is important to extract optimal building primitives that satisfy the geometric condition for building and are representative of the existing large scale 3D buildings scene. To extract optimal building primitives, priority function is defined based on the orientation of buildings, number of boundary lines or polygons describing the building, type of buildings, and inner angles between building lines (Equ. 1). The buildings having the minimum value of the priority function are selected to be used in the registering process.

$$M_i = \arg\min_{\forall\{M_i\}_{i=1,2\sim,N}} S_M\big[M_i(D, N_L, N_P, P_t, I_\theta)\big] \qquad (1)$$

where, M_i denotes building model and S_M is the priority function to extract optimal building primitive. D, N_L, N_P, P_t and I_θ denote orientation of building, number of boundary

lines, number of polygons, building type, and inner angles between building vectors, respectively.

2.1.2   Extraction of image straight lines primitives

Although many line detectors have been introduced, the Burns algorithm (Burns et al., 1986) is selected for our research because the line data extracted by the algorithm include the representative line and its length, contrast, width, location, orientation and straightness. There are three steps to the Burns algorithm in this study. Pixels are grouped into line-support regions based on the similarity of the gradient orientation. This allows for data-derived organization of edge contexts without committing to a particular size. To group the pixels into line-support regions, the connected-components algorithm proposed by Lumia et al., 1983 is used. In the next step the image intensity slope surface is approximated by a planar surface. The planar fit is weighted by the gradient magnitude associated with the pixels so that intensities in the steepest part of the edge will dominate. Finally, straight lines are extracted by computing the intersection between the planar fit and the horizontal surface in each line-support region. As mentioned above, these straight lines have geometric information such as the coordinates of start and end points and attributes of the parameters of lines.

2.2 Domain of comparison

The extracted optimal building models are in the object space while the image straight lines are located in the image space. For comparing both primitives, the optimal building models and the image straight lines should be in the same domain. Therefore, the optimal building models are projected into image space by the collinearity equations using the camera interior orientation parameters and the initial camera exterior orientation parameters obtained by the GPS and IMU sensors. Consequently, the similarity measurement, and thus the matching of primitives, is carried out in the image space.

2.3 Similarity measurement and primitives matching

Due to errors in the initial EO parameter, and geometric errors in the existing 3D building models, the optimal building primitives projected into image space do not correspond with the straight lines extracted in image. In this study, we assume that the existing 3D building models are error-free and the errors are only with the initial EO parameters. Similarity measurement is required for extracting new image coordinates for the optimal building primitives by measuring the relationship between optimal building primitives and image straight lines in the image space. The process of similarity measurement begins by scoring the sum of image line length contained in the buffer zone of the projected vectors comprised of optimal building primitives against the optimal building primitives placed in the designated image area. The image location having the highest score is selected as the image coordinates corresponding to the optimal building primitives. In this location, new image straight lines are extracted by weighing the straight lines representing each vector of optimal building primitives. The intersection points are computed from the new lines and then the points are considered as corresponding image coordinates of the optimal building primitives. Figure 2 shows the proposed method for similarity measurement.
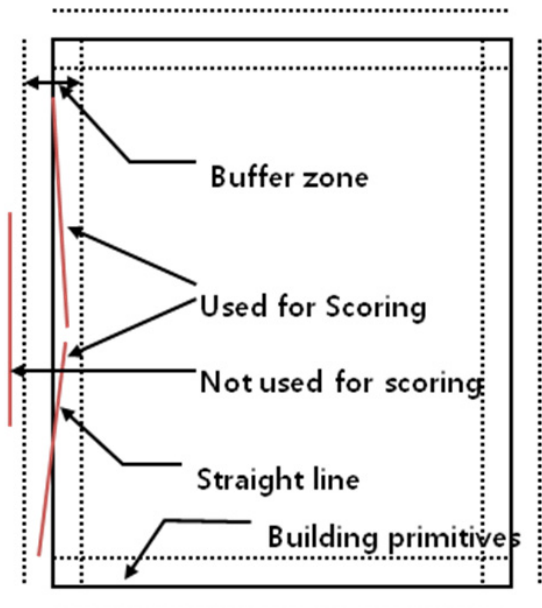
In: Wagner W., Székely, B. (eds.): ISPRS TC VII Symposium – 100 Years ISPRS, Vienna, Austria, July 5–7, 2010, IAPRS, Vol. XXXVIII, Part 7B

Contents   Author Index   Keyword Index

Figure 2. Similarity measurement

2.4 Adjustment of EO parameters

The EO parameters of the image are adjusted through space resection using pairs of the object coordinates (X, Y, Z) of optimal building primitives and their newly derived image coordinates (x, y) derived in the similarity measurement process.

3. RESULTS

3.1 Test data

The testing of the method was carried out in a study area of York University in Toronto. Existing 3D building models and an aerial colour image acquired in 2009 provided by First Base Solution were used in the study. Figure 3 shows the existing 3D building models and aerial image used in this study.
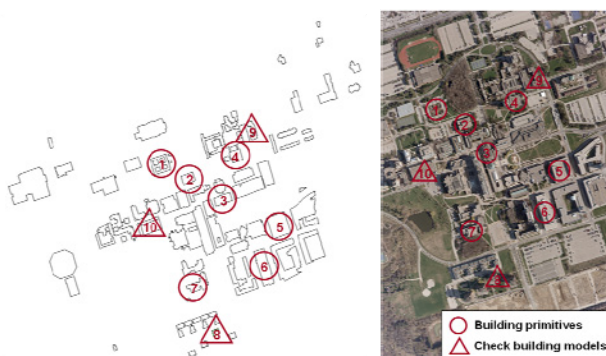

Figure 3. Existing 3D building models and the aerial image

3.2 Feature extraction

A total of 7 optimal building primitives were selected by analysing the orientation of building, complexity of building, inner angles of building, and geometric building type in the study area. Six of the seven optimal building primitives are rectangular and the seventh is hexagon with inner angles of 90 degrees. As well, we can see that the principal axes of the

optimal building primitives point to the same direction. The circles in Figure 3 show shape and distribution of the extracted optimal building primitives. 3 building models indicated by the triangles in Figure 3 are selected as check buildings to evaluate the accuracy of alignment. Straight lines corresponding to the optimal building primitives are extracted in image by the Burns algorithm. Straight lines having a length of less than 3m of the entire extracted straight lines are removed for effective

Figure 4. Extracted straight primitives (building 1)
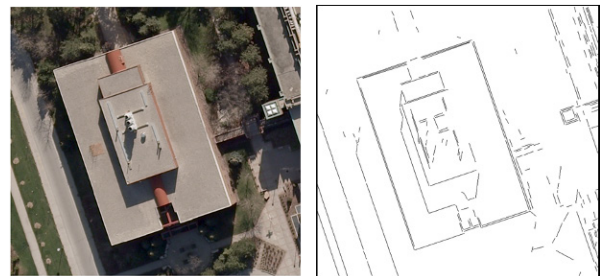

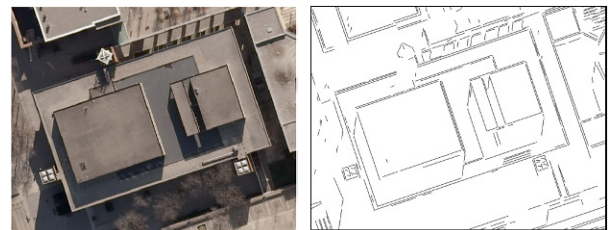Figure 5. Extracted straight primitives (building 2)

Figure 6. Extracted straight primitives (building 3)

Figure 7. Extracted straight primitives (building 4)

Figure 8. Extracted straight primitives (building 5)

In: Wagner W., Székely, B. (eds.): ISPRS TC VII Symposium – 100 Years ISPRS, Vienna, Austria, July 5–7, 2010, IAPRS, Vol. XXXVIII, Part 7B

Contents   Author Index   Keyword Index

Figure 9. Extracted straight primitives (building 6)

Figure 10. Extracted straight primitives (building 7)

Figure 11. Results of back projecting into image space

Figure 12. Enlarged image of back–projected building 4

registration process. Figures 4 to 10 show the results of extracted straight lines primitives for each building in the image.

3.3 Back projection

Optimal building primitives were back projected into image space and figure 11 illustrates the result of each building. Figure 12 shows a closed-up view of the back-projection on the image of building 4. In this figure, the red lines represent the optimal building primitives. Column 2 in Table 1 presents the image coordinates of the optimal building primitives after back projecting them into image space. The back projection results show that there is a small difference in the image coordinates between optimal building primitives projected into image and the building image because of errors contained in the initial EO parameters.

3.4 Similarity measurement and matching

Similarity measurement was carried out with a 10 pixel buffer zone in search area. 30 pairs of coordinates corresponding to the vertices of the optimal building primitives are automatically obtained by computing the intersections of the new straight lines after finding new location of optimal building primitives. Table 1, column 3, shows the results of image coordinates corresponding to the extracted optimal building primitives.

Table 1. Quantitative assessment with optimal building primitives

	Optimal building primitives (Object space)			Image coordinates extracted manually(1)		Coordinates of Building primitives projected into image space(2)		Automatically extracted coordinates by similarity measurement(3)	
	X(m)	Y(m)	Z(m)	X(pixel)	Y(pixel)	X(pixel)	Y(pixel)	X(pixel)	Y(pixel)
Building 1	620217.24	4848040.89	167.15	2916	5547	2921.22	5544.96	2915.14	5544.35
	620146.18	4848017.03	167.15	3098	6094	3103.56	6091.23	3098.17	6092.96
	620168.29	4847951.20	167.16	3604	5925	3609.60	5922.73	3607.72	5923.29
	620239.31	4847975.04	167.16	3425	5380	3427.44	5376.69	3424.78	5374.92
Building 2	620285.81	4847945.87	175.68	3635	5032	3640.03	5027.56	3634.55	5031.68
	620297.64	4847909.79	175.74	3915	4939	3919.02	4936.86	3914.40	4940.70
	620350.87	4847927.55	174.70	3778	4526	3783.92	4524.45	3778.02	4524.42
	620338.85	4847963.57	175.75	3498	4619	3503.87	4617.28	3497.11	4617.53
Building 3	620386.56	4847837.71	174.96	4476	4252	4478.37	4250.46	4475.77	4251.39
	620406.61	4847776.84	175.01	4951	4096	4949.13	4096.63	4952.36	4095.65
	620442.84	4847788.77	175.05	4858	3814	4857.49	3816.35	4860.45	3814.55
	620422.79	4847849.64	174.82	4384	3970	4386.87	3970.20	4384.00	3970.30
Building 4	620550.63	4848063.44	169.83	2739	2980	2746.82	2980.75	2738.37	2980.45
	620504.54	4848048.32	169.88	2855	3336	2862.55	3336.07	2854.51	3337.03
	620519.95	4848002.25	169.96	3209	3218	3217.41	3218.14	3208.79	3219.29
	620565.94	4848017.63	169.92	3092	2863	3099.65	2863.53	3090.62	2863.43
Building 5	620753.79	4847797.58	176.63	4795	1406	4793.49	1408.54	4794.11	1407.82
	620675.77	4847771.87	176.59	4992	2008	4991.26	2013.39	4990.29	2007.80
	620705.72	4847682.57	176.74	5682	1777	5683.18	1782.69	5680.77	1777.59
	620783.60	4847708.69	176.61	5482	1178	5482.31	1179.05	5481.51	1178.80
Building 6	620563.73	4847602.66	188.92	6306	2872	6304.02	2876.78	6307.17	2872.21

In: Wagner W., Székely, B. (eds.): ISPRS TC VII Symposium – 100 Years ISPRS, Vienna, Austria, July 5–7, 2010, IAPRS, Vol. XXXVIII, Part 7B

Contents   Author Index   Keyword Index

	620590.78	4847522.45	189.85	6934	2662	6931.69	2666.24	6934.84	2661.68
	620604.89	4847527.20	188.93	6896	2553	6894.12	2556.62	6897.14	2551.67
	620577.84	4847607.41	189.07	6270	2763	6267.26	2766.40	6270.27	2761.45
Building 7	620309.61	4847485.66	177.48	7205	4856	7200.85	4853.73	7205.98	4855.24
	620315.47	4847468.22	177.51	7346	4808	7336.08	4808.71	7342.80	4809.70
	620327.47	4847472.26	177.55	7309	4716	7305.08	4715.75	7307.08	4715.75
	620333.49	4847454.58	177.49	7446	4668	7442.09	4669.44	7444.98	4669.81
	620374.30	4847468.44	177.52	7342	4352	7335.62	4353.18	7338.15	4352.52
	620362.97	4847503.61	177.54	7067	4439	7062.97	4440.27	7067.20	4439.07
Compared to image coordinates extracted manually				Average (pixel)		1.07	0.52	-0.43	-0.23
				RMSE(pixel)		4.55	2.62	1.62	1.43

3.5 Adjustment of EO parameters

With the 30 pairs of building model primitives and their image coordinate extracted by similarity measurement, the EO parameters are adjusted in a least squares solutions as shown in table 2.

Table 2. Adjusted EO parameters

	Initial EO parameter	Adjusted EO parameter
X(m)	620455.282	620454.647
Y(m)	4847674.264	4847676.303
Z(m)	1632.24	1629.578
Omega(deg)	0.06556	-0.01266
Phi(deg)	0.14135	0.12273
Kappa(deg)	-89.86594	-89.88080

3.6 Assessment of the proposed method

In order to evaluate the performance of the proposed method, qualitative and quantitative assessments were carried out with both optimal and check building models, respectively. Both optimal and check building models are back-projected into image space using the adjusted EO parameters. Figure 13 shows the results of each optimal building projected into image space after the EO parameters are adjusted, and Figure 14 shows better matching of the building edges using the new EO parameters than the initial EO parameters when compared to Figure 12. Reference coordinates corresponding to optimal and check building models were also manually extracted from the image for quantitative assessments (Table 1, column (1) and Table 2, column (1)). The reference coordinates are compared to coordinates of optimal building automatically extracted in Table 3. While the results with initial EO parameters show that the average difference in X and Y directions are 1.07 and 0.52 pixels

respectively, with RMSE of 4.55 and 2.66 pixels respectively, the results with the new EO parameters show that the average differences in X and Y directions are 0.43 and 0.23 pixels, with RMSE of 1.62 pixel and 1.43 pixels, respectively. The test is also carried out in a similar manner with check building models which were not used in the registration process. The average coordinate differences of check building models with initial EO parameters were 0.42 and 0.13 pixels in X and Y directions, with RMSE of 4.99 and 2.66 pixels, respectively. After adjusting the EO parameters, the result show that the average differences in X and Y direction are 0.45 and 0.59 pixels, with RMSE of 0.66 and 1.49 pixels, respectively.

Figure 13. Back-projection results after adjusting EO parameters

Figure 14. Enlarged image of the back-projected Building 4 using the new EO parameters

Table 3. Quantitative assessment with check buildings

	Check building vectors			Image coordinates of check buildings extracted manually(1)		Image coordinates of check buildings obtained by initial EO parameters		Image coordinates of check buildings obtained by automatically adjusted EO parameters	
	X(m)	Y(m)	Z(m)	X(pixel)	Y(pixel)	X(pixel)	Y(pixel)	X(pixel)	Y(pixel)
Building 8	620426.84	4847296.02	196.82	8717	3951	8712.04	3952.48	8717.21	3950.73
	620434.24	4847273.58	197.00	8894	3894	8888.84	3894.82	8894.19	3892.93

In: Wagner W., Székely, B. (eds.): ISPRS TC VII Symposium – 100 Years ISPRS, Vienna, Austria, July 5–7, 2010, IAPRS, Vol. XXXVIII, Part 7B

Contents   Author Index   Keyword Index

	620462.35	4847283.10	196.90	8820	3673	8814.52	3673.92	8819.71	3671.72
	620454.97	4847305.51	196.97	8644	3731	8638.47	3731.46	8643.48	3729.39
Building 9	620583.17	4848170.14	174.48	1906	2726	1913.42	2725.02	1904.89	2722.50
	620606.54	4848099.71	174.47	2452	2543	2457.80	2545.60	2450.69	2542.62
	620633.01	4848108.29	174.30	2385	2338	2392.24	2340.99	2384.92	2337.57
	620609.43	4848178.84	174.35	1840	2519	1846.87	2522.00	1838.13	2519.04
Building 10	620084.29	4847745.74	178.76	5183	6598	5182.56	6594.73	5182.64	6599.30
	620102.43	4847691.31	178.71	5605	6461	5604.51	6455.31	5605.40	6459.34
	620202.51	4847724.94	178.53	5346	5683	5345.80	5679.46	5345.98	5682.09
	620184.17	4847779.22	178.67	4925	5821	4924.96	5820.60	4924.32	5823.72
Compared to image coordinates extracted manually			Average(pixel)			0.42	-0.13	-0.45	-0.59
			RMSE(pixel)			4.99	2.66	0.66	1.49

4. CONCLUSIONS

In this study, we present a new method for registering existing 3D building models with image data. Optimal building models are extracted with a priority function using information of 3D building model. Straight lines in the image are also extracted by the Burns algorithm. Optimal building primitives are projected into image space to compare both sets of data. Corresponding coordinate pairs are computed by similarity measurement, scoring straight lines contained in the buffer zone of the optimal building model. Finally, computed coordinates pairs are used to adjust the initial EO parameters. The proposed method for registering 3D building models with image data has been tested. The experiment showed that with optimal building models average differences of 0.43 pixel and RMSE of 1.62 pixel in the X direction and of average difference of 0.23 pixel and RMSE of 1.43 pixel in the Y direction were obtained. For the check building models the results were 0.43 pixel with RMSE of 0.66 pixel in the X direction and 0.59 pixel with RMSE of 1.49 pixel in the Y direction. These results indicate that our proposed data-driven method can effectively register and align existing 3D building models with new acquired image data. Further work is needed to improve the proposed method by considering and including the errors of 3D building models and estimate their impact in the registration process.

ACKNOWLEDGEMENT

REFERENCES

Burns, J. B., Hanson, A. R. and Riseman, E. M., 1986. Extracting Straight Lines. *IEEE Trans. Pattern Analysis and Machine Intelligence*, Vol. 8, pp. 425-445.

Fonseca L, M. G. and Manjunath B. S., 1996. Registration Techniques for Multisensor Remotely Sensed Imagery. *Photogrammetric Engineering & Remote Sensing,* Vol. 62, No. 9, pp. 1049-1056.

Habib, A., Ghanma, G., Morgan, M., and Al-Ruzouq, R., 2005. Photogrammetric and Lidar Data Registration Using Linear Features. *Photogrammetric Engineering & Remote Sensing*, Vol. 71, No. 6, pp. 669-707.

Lumia, R., Shapiro. L. and Zuniga, O., 1983. A New Connected Components Algorithm for Virtual Memory Computers. *Computer vision, Graphics, and Image Processing*, Vol. 22, pp. 287-300.

Zitova, B. and Flusser, J., 2003. Image registration method: a survey. *Image and Vision Computing*, Vol. 21, pp. 977-1000.